The Effect of Rock Constitutive Model on Stability and Deformation in Tunnel Design

Muhammad Hafizh Muhsin Amin[1]*, Herwan Dermawan[1]
[1]Civil Engineering Study Program, Indonesia University of Education

*Corresponding Author: Muhammad Hafizh Muhsin Amin. Email: hafizhmuhsin@upi.edu

ORCID: Muhammad Hafizh Muhsin Amin. https://orcid.org/0009-0009-2012-8646

Abstract

Numerical analysis using the Finite Element Method (FEM) is standard for assessing tunnel stability, but its accuracy depends heavily on the chosen rock constitutive model and analysis dimension (2D vs. 3D). Significant discrepancies between 2D and 3D results, not yet fully quantified across models, pose a considerable risk as simplified 2D analyses can lead to unsafe estimations of structural loads. This study systematically compares the Mohr-Coulomb (M-C), Hoek-Brown (H-B), and Drucker-Prager (D-P) models using 2D and 3D FEM simulations. A standard horseshoe tunnel was analyzed for deformation, factor of safety (FoS), internal forces, and sensitivity to key parameters. Key findings reveal 3D analysis predicts substantially higher loads, with liner axial forces up to 25 times greater than 2D predictions due to the 3D arching effect. Model choice is more critical in 3D, where M-C yielded liner forces 30% higher than H-B. The H-B model showed greater sensitivity, predicting lower stability in the 2D analysis. This research provides quantitative evidence that 2D plane-strain analysis is unsafe for final design as it massively underestimates peak loads. The findings offer engineers practical guidance on the quantitative impact of model selection in a 3D context, contributing to safer, more reliable tunnel engineering practices.

Keyword: Tunnel, rock mechanics, constitutive models, rock mass strength, finite element method

1 INTRODUCTION

Tunnel stability and deformation are crucial aspects of geotechnical engineering whose success is largely determined by an accurate understanding of the interaction between the rock mass and the support system. Numerical analysis using the Finite Element Method (FEM) has become a standard approach to predict the behavior of rock masses during and after excavation. However, the reliability of such predictions is highly dependent on the selection of a constitutive model that represents the rock stress-strain relationship. The common models, such as Mohr-Coulomb (M-C), Hoek-Brown (H-B), and Drucker-Prager (D-P), have different assumptions and mathematical frameworks, resulting in varying predictions (1,2).

Previous studies have confirmed that the use of a constitutive model significantly affects the stability analysis results, including the factor of safety and stress distribution around the tunnel (3,4). In addition, the sensitivity of the analysis results to geotechnical parameters such as initial stress conditions and rock mass characteristics has also been identified as a determining factor (5,6) Nonetheless, some significant research gaps still exist. First, the majority of studies tend to apply one type of constitutive model without conducting comprehensive performance comparisons under diverse geotechnical conditions. Second, the analysis is often limited to 2D approaches, which lack the ability to capture the complexity of three-dimensional deformation in heterogeneous rock masses. Third, the influence of geotechnical parameter uncertainty on the analysis results of different constitutive models has not been explored in depth.

To overcome this gap, this study aims to present a systematic comparative analysis to evaluate the effect of Mohr-Coulomb, Hoek-Brown, and Drucker-Prager constitutive models on tunnel stability and deformation. Using FEM modeling in 2D and 3D configurations, this study will specifically: (1) measure the differences in deformation predictions and factors of safety between models under various geotechnical scenarios, and (2) integrate uncertainty analysis to assess the reliability of each model. The results of this study are expected to provide practical guidance for engineers in selecting the most suitable constitutive model, so as to improve accuracy and safety in tunnel design.

1.1 Mohr-Coulomb Model (MC)

Mohr's theory assumes that for a stress state σ1 > σ2 > σ3, the intermediate stresses do not affect rock collapse, and tensile strength is not equal to compressive strength. This theory is based on the assumption that normal stress and shear stress acting on the sliding plane play the most role in the rock collapse process (7). In terms of rock mechanics, the Mohr-Coulomb model involves rock mass shear strength values that are determined based on the equivalent cohesion and shear angle values between the Mohr-Coulomb and Hoek-Brown models (4).

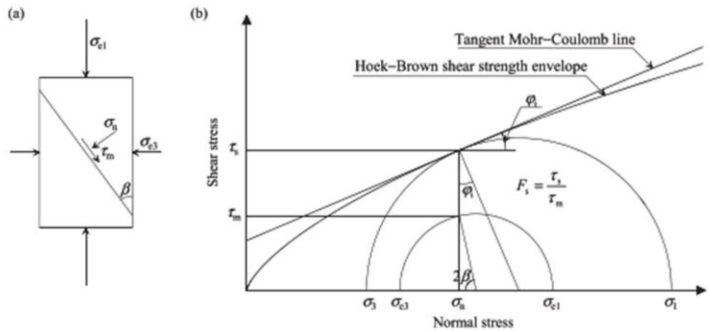

Figure 1. Stress diagram of Mohr-Coulomb model

The values of the parameters c and φ are obtained by fitting the relationship between the minor-major principal stress values of the rock. The results of these equations for the values of c and φ are as follows:

$$\phi' = \sin^{-1}\left[\frac{6am_b(s+m_b\sigma'_{3n})^{a-1}}{2(1+a)(2+a)+6am_b(s+m_b\sigma'_{3n})^{a-1}}\right] \quad \text{1.1}$$

$$c' = \left(\sigma_{ci}\left[(1+2a)s+(1-a)m_b\sigma'_{3n}\right](s+m_b\sigma'_{3n})^{a-1}\right) \Big/ \left[(1+a)(2+a) \times\sqrt{1+(6am_b(s+m_b\sigma'_{3n})^{a-1})/((1+a)(2+a))}\right] \quad \text{1.2}$$

1.2 Hoek-Brown Model (HB)

The Hoek-Brown criterion is an empirical criterion derived from an equation that fits statistically to a data set obtained from test results. Hoek & Brown proposed a method to calculate the strength of rock masses with discontinuous planes. The use of this collapse criterion for very poor quality rock masses uses the Geological Strength Index (GSI) rock mass classification (7).

$$\sigma_1' = \sigma_3' + \sigma_{ci}\left(m_b\frac{\sigma_3'}{\sigma_{ci}}+s\right)^a \quad \text{1.3}$$

Where *mb* is the reduced value of the material constant, while the values of *s* and *a* are constants for the rock mass obtained from the following equation:

$$m_b = m_i \exp\left(\frac{GSI-100}{28-14D}\right) \quad \text{1.4}$$

$$s = \exp\left(\frac{GSI-100}{9-3D}\right) \quad \text{1.5}$$

$$a = \frac{1}{2} + \frac{1}{6}\left(e^{-GSI/15} - e^{-20/3}\right) \quad \text{1.6}$$

Meanwhile D is a factor that depends on the disturbance degree of the rock mass that was damaged during construction by blasting. Its value varies between 0 - 1 (8)

1.3 Drucker-Prager Model (DP)

The Drucker-Prager model offers significant advantages in the implementation of the finite element method (FEM). Its main characteristics are a smooth yield surface and no singularity points (corners), which results in higher numerical stability and reduced convergence problems in the analysis. The Drucker-Prager criterion can be considered as a failure criterion that indicates the mechanical strength of brittle materials. This failure criterion can be expressed as:

$$\sqrt{J_2} = \lambda I_1' + \kappa \quad \text{1.7}$$

Where k and λ are material constants and J_2 is the second invariant of the deviator stress tensor and $I`_1$ is the first invariant of the stress tensor. The parameters λ and k can be determined from the triaxial test results and can be expressed in terms of inner shear angle and cohesion as follows:

$$I_1' = \sigma_1' + \sigma_2' + \sigma_3'$$
$$J_2 = \frac{1}{6}\left[(\sigma_1' - \sigma_2')^2 + (\sigma_1' - \sigma_3')^2 + (\sigma_3' - \sigma_1')^2\right] \quad \text{1.8}$$

$$\lambda = \frac{2\sin\phi}{\sqrt{3}\,(3-\sin\phi)} \quad \text{1.9}$$

$$\kappa = \frac{6c\cos\phi}{\sqrt{3}\,(3-\sin\phi)} \quad \text{1.10}$$

The Drucker-Prager failure criteria parameters can also be calculated based on the Mohr-Coulomb strength parameters as follows:

$$q = \frac{\sin\phi}{\sqrt{1+\frac{1}{3}\sin^2\phi}} \quad \text{1.11}$$

$$k = \frac{c\cos\phi}{\sqrt{1+\frac{1}{3}\sin^2\phi}} \quad \text{1.12}$$

2 METHOD

This research aims to analyze the effect of rock constitutive models on stability and deformation in tunnel design. The research focused on comparing the analysis results using several constitutive models, specifically Mohr-Coulomb and Hoek-Brown, and Drucker-Prager under certain rock conditions. The analysis was conducted using finite element modelling (FEM) in two-dimensional (2D) and three-dimensional (3D) configurations to obtain a comprehensive comparison.

2.1 Model Building

The tunnel model analyzed has a horseshoe geometry with dimensions of 9.4 meters wide and 9.4 meters high. This configuration represents a common design in underground infrastructure projects. To ensure stability, the tunnel was modelled with a support system consisting of: Steel Ribs: 20x20 cm steel profiles; Shotcrete: Two layers of sprayed concrete with a total thickness of 3 cm (2 x 1.5 cm), reinforced with wiremesh; Rockbolts: Rock bolts with a length of 5 meters installed with a spacing of 1 meter. All these components of the support system were integrated into the numerical model to realistically simulate the rock-buffer interaction.

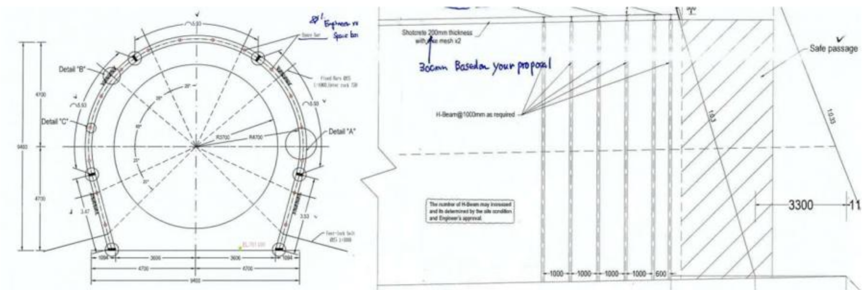

Figure 2. Cross section and typical long section of tunnel

2.2 Numerical Modelling and Analysis Procedures

Numerical analysis is conducted in two different software platforms to accommodate both 2D and 3D analysis: 2D analysis: a finite element program specifically designed for stress-strain and stability analysis in underground excavations; 3D analysis: modelling soil and rock behaviour in complex three-dimensional conditions. The analysis procedure for each modelling follows the following steps:

1. Initialization of Initial Conditions: Determining the in-situ stress conditions (initial stresses) in the rock mass prior to excavation.
2. Excavation Simulation: Simulating the tunnel excavation process.
3. Support System Installation: Activates the support system elements (shotcrete, steel ribs, and rockbolts) in the model.
4. Comparative Analysis: Runs an analysis using three different constitutive models (e.g., Mohr-Coulomb, Hoek-Brown, and Drucker-Prager) on the same model to compare the results.

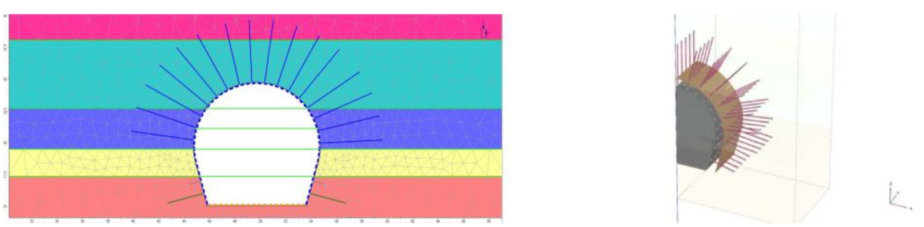

Figure 3. Tunnel models for numerical analysis

2.3 Output and Evaluation Criteria

To evaluate the effect of each constitutive model, three main output parameters were analyzed:

1. Tunnel Stability: Measured based on the Factor of Safety (FoS) or Strength Reduction Factor (SRF) obtained from the analysis.
2. Rock Mass Deformation: Includes analysis of total displacement and vertical deformation (settlement) around the crown and walls of the tunnel.
3. Internal Force on Support Elements: Analyzes the magnitude of axial forces and bending moments acting on the steel ribs, shotcrete, and rockbolts elements.

The results of these three parameters are then systematically compared to identify the characteristics, advantages and limitations of each constitutive model in the context of tunnel design.

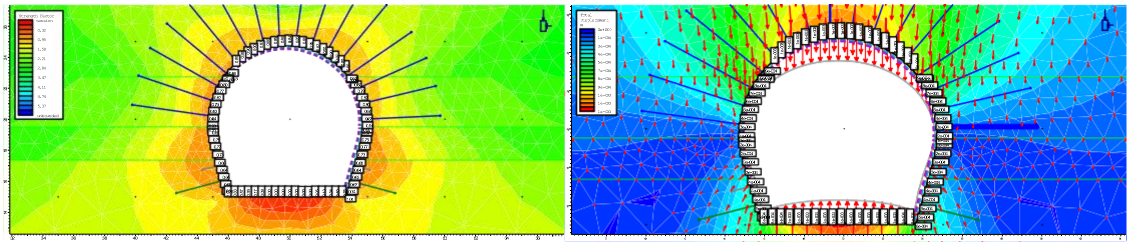

Figure 4. Analysis results for evaluation

2.4 Soil Parameters

The soil parameter around the tunnel model were calculated from field investigation data using empirical correlation method.

Table 1. Soil Parameters

Layer	γ	Em	ν	σ_T	σ_{ci} (UCS)
	kN/m3	GPa		MPa	MPa
1	17	0.002	0.4		
2	24.05	3.605	0.097	1.3	13
3	24.65	5.477	0.070	3	30
4	24.05	3.605	0.097	1.3	13
5	26.8	5.916	0.068	3.5	35
6	24.4	4.591	0.12	6.67	66.67

Table 2. Hoek-Brown Criterion

Layer	mi	GSI	mb	a	s
1	-	-	-	-	-
2	21	50	3.521	0.506	0.0039
3	22	50	3.689	0.506	0.0039
4	21	50	3.521	0.506	0.0039
5	22	50	3.689	0.506	0.0039
6	19	40	2.229	0.511	0.0013

Table 3. Mohr-Coulomb and Drucker-Prager Criterion

Layer	MB		DP	
	c	phi	q	k
	MPa	°		MPa
1	-	-	-	-
2	0.2218	53.53	0.48	1.08
3	0.3273	59.27	0.48	2.49
4	0.2218	53.53	0.48	1.08
5	0.3683	59.71	0.48	2.90
6	0.3604	60.74	0.73	3.49

2.5 Structures Parameters

The parameters used as the basis for force analysis in tunnel reinforcement systems are as follows.

Table 4. Shotcrete calculation parameters

E (kPa)	γ (kN/m^3)	d (mm)	ν
8,27, E+05	24	15	0,2

Table 5. Steelrib calculation parameters

E (kPa)	γ (kN/m^3)	d (mm)	ν
2,10, E+08	78,5	0,2	0,3

Table 6. Rockbolt calculation parameters

E (kPa)	γ (kN/m^3)	D (mm)	T_{skin} (kPa)
2,10, E+08	78,5	25	393

3 RESULTS AND DISCUSSION

3.1 Analysis of deformation results

Table 7. Analysis of deformation results of different models and analysis type

No.	Stage	Max Displacement (mm)	
		MC	HB
1	2D	1.272	1.271
2	3D 5 m	0.966	0.885
3	3D 10 m	1.280	1.126
4	3D 15 m	1.461	1.297
5	3D 20 m	1.647	1.516

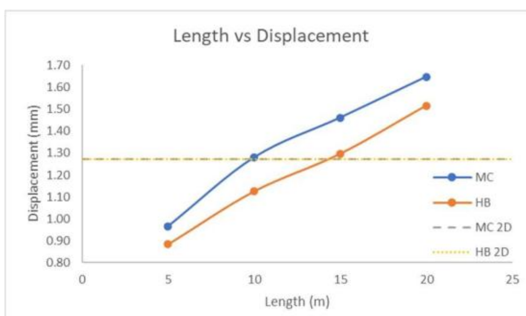

Figure 5. Comparison of deformation results of different models and analysis type

The data shows that 2D simulations tend to give slightly higher deformation values than 3D simulations at initial excavation lengths, but this trend reverses at longer excavations. This trend shows that the three-dimensional effect plays a role in distributing stress more efficiently in short excavations, but the effect is reduced in long excavations due to the accumulation of deformation.

3.2 Analysis of stability and safety factor results

Table 8. Analysis of stability results of different models and analysis type

No.	Stage	Max Displacement (mm)		Safety Factor	
		MC	HB	MC	HB
1	2D	1.272	1.271	0.800	0.001
2	3D 5 m	0.966	0.885	5.788	2.966
3	3D 10 m	1.280	1.126	5.588	2.548
4	3D 15 m	1.461	1.297	4.525	2.445
5	3D 20 m	1.647	1.516	4.289	2.227

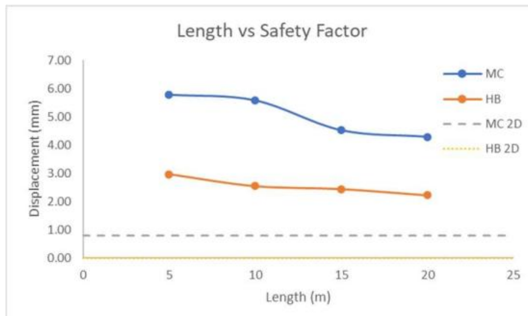

Figure 6. Comparison of safety factor results of different models and analysis type

The results of analyses shows that the safety factor of 2D is significantly lower, especially in the Hoek-Brown model which shows a value of SF = 0 in the 2D condition, indicating a numerical total failure or unstable condition that is not conservatively predicted by the 2D model. In conclusion, the 3D model provides more realistic and stable results than the 2D model in assessing the deformation performance and tunnel stability, especially when used at significant excavation lengths.

3.3 Analysis of internal forces of the tunnel support system

Table 9. Analysys of internal forces of different models and analysis type

Model	Rockbolt Axial Force (kN)	Rockbolt Axial Stress (MPa)	Liner Axial Force (kN)	Liner Bending Moment (kNm)	Liner Shear Force (kN)
Mohr-Coulomb	3.88	7.91	109.46	7.45	29.14
Hoek-Brown	3.89	7.93	108.82	2.63	10.27
Drucker-Prager	3.89	7.93	108.82	2.63	10.27

Model	Rockbolt Axial Force (kN)	Rockbolt Shear Force (kN)	Rockbolt Bending Moment (kNm)	Rockbolt Skin Friction (kN)	Liner Axial Force (kN)	Liner Shear Force (kN)	Liner Bending Moment (kNm)
Mohr-Cou	176.60	23.59	0.008	393	2649.00	219.80	76.97
Hoek-Brov	44.59	2.367	0.063	320.1	1965.00	228.00	46.07

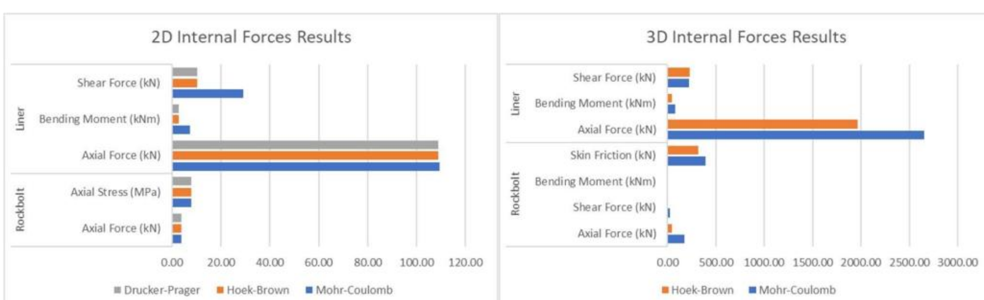

Figure 7. Internal forces analysis results of different models

The results of the internal force analysis showed significant differences between 2D and 3D simulations for both rockbolt and liner elements. The 3D analysis consistently resulted in higher values of axial force, shear force, and bending moment because it accounted for the spatial contribution along the tunnel length, in contrast to the 2D approach that only evaluated cross-sectional conditions. This indicates that the 3D approach not only provides more realistic results, but is also more sensitive to the behaviour of the structure under complex spatial load distributions. Therefore, it is more appropriate to use the 2D analysis as a preliminary or estimation approach, while the final design is strongly recommended to refer to the 3D simulation results.

3.4 Analysis of the effect of various rock parameters

This analysis was performed to evaluate the effect of certain parameter variations on the deformation response and stability of the tunnel. In this simulation, sensitivity was tested for key parameters that apply across the constitutive model, specifically the initial stress ratio (K_0) and Uniaxial Compression Strength (UCS).

3.4.1 Initial Stress Ratio (K_0)

In this study, the initial stress ratio value was variated with the assumption that the vertical stress is determined from the depth of the tunnel and the unit weight of the rock, while the horizontal stress is varied according to the ratio.

Table 10. Initial stress ratio variation analysis results

Initial Stress Ratio										
No.	K0	Displacement (mm)			Min Strength Factor			Max Strength Factor		
		MC	HB	DP	MC	HB	DP	MC	HB	DP
1	0.33	1.3796	1.3834	1.3834	0.4	0.01	0.59	2.18	0.86	3.05
2	0.5	1.2717	1.2706	1.2706	0.84	0.17	0.63	1.71	1.01	2.31
3	0.75	1.2031	1.2021	1.2021	0.87	0.47	0.7	1.52	1.13	1.47
4	1	1.1345	1.1337	1.1337	0.89	0.65	0.8	1.54	1.15	1.36
5	1.25	1.2411	1.2438	1.2438	0.9	0.7	0.85	1.53	1.13	1.29
6	1.5	1.5785	1.5894	1.5894	0.91	0.73	0.89	1.5	1.11	1.39
7	2	2.3041	2.3138	2.3138	0.85	0.7	0.81	1.46	1.12	1.26
8	3	3.7561	3.7635	3.7635	0.73	0.58	0.6	1.38	1.11	1.22

According to the simulation results, it can be seen that the higher the initial stress ratio value, the more deformation occurs and the strength factor increases. This indicates that the horizontal stress contributes to deformation restraint and a more even stress redistribution around the tunnel opening.

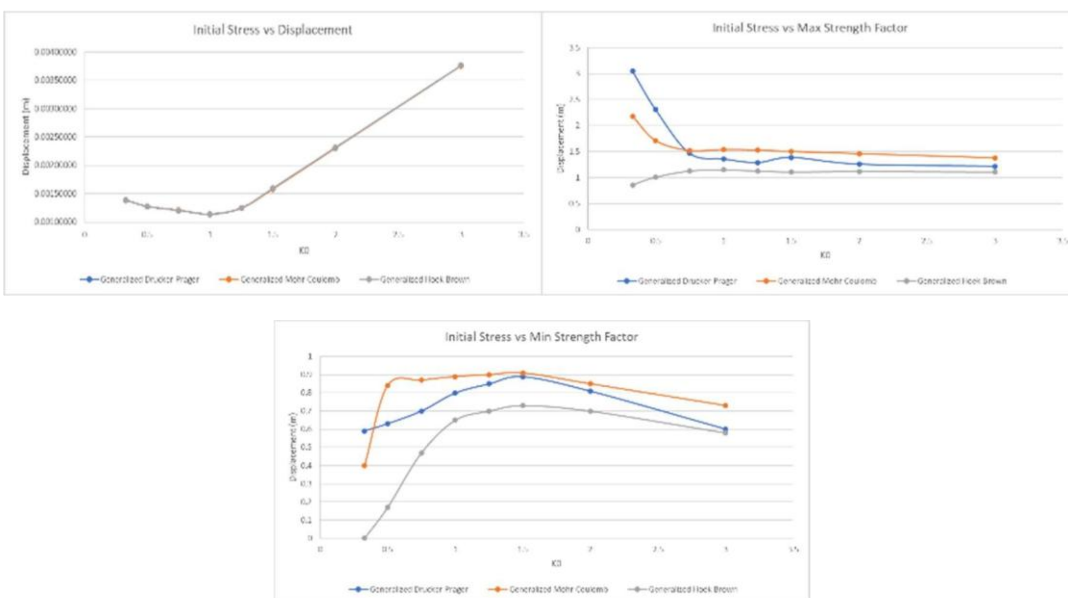

Figure 8. Analysis results of the effect of K0 condition on different models

3.4.2 Uniaxial Compressive Strength (UCS)

Uniaxial compressive strength (UCS) or σ_{ci} is a basic parameter that reflects the strength of intact rock to axial loading without lateral influence. Variations in σ_{ci} values can have a significant impact on numerical simulation results, both in terms of deformation and stability. In this analysis, σ_{ci} is varied into three values, which are low, medium and high from 10 MPa to 100 MPa, representing weak to medium-strong rock conditions.

Table 11. UCS variation analysis results

No.	UCS (MPa)	Uniaxial Compression Strength								
		Displacement (mm)			Min Strength Factor			Max Strength Fact		
		MC	HB	DP	MC	HB	DP	MC	HB	DP
1	10	2.148	2.148	2.148	0.81	0.1	0.65	1.38	1.21	1.29
2	15	1.753	1.753	1.753	0.86	0.17	0.67	1.45	1.25	1.34
3	20	1.517	1.517	1.517	0.9	0.22	0.7	1.5	1.28	1.4
4	30	1.237	1.237	1.237	0.95	0.31	0.74	1.58	1.31	1.5
5	40	1.071	1.071	1.071	1	0.37	0.76	1.65	1.34	1.55
6	50	0.957	0.957	0.957	1.03	0.44	0.78	1.72	1.37	1.6
7	75	0.780	0.780	0.780	1.11	0.6	0.83	1.87	1.43	1.74
8	100	0.675	0.675	0.675	1.18	0.73	0.88	2.01	1.48	1.88

The simulation results show that increasing the UCS value significantly decreases the maximum deformation occurring at the tunnel crown, and conversely increases the local strength factor value. The deformation pattern is more concentrated and the plastic zone is narrower at high σ_{ci} values, indicating that rocks with high strength are better able to resist stress redistribution due to excavation.

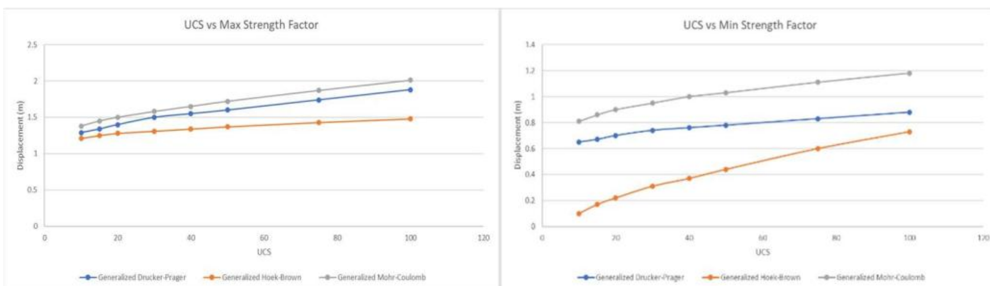

Figure 9. Analysis results of the effect of UCS parameters on different models

4 CONCLUSION

This study examines the effect of three different constitutive models on stability and deformation in tunnel design using 2D and 3D finite element method analysis that calculates deformation magnitude, factor of safety, and stress distribution by considering the effects of varying UCS parameters and initial stress ratio. This leads to the following conclusions:

1. The HB model that takes into account the rock mass and discontinuous plane conditions generated more sensitive stability and deformation values than the other constitutive models. The maximum stresses are distributed at the roof and bottom of the tunnel.
2. Compared to the HB model, the MC model produced larger displacement values with a maximum difference of 0.72% in the 2D analysis and 13.68% in the 3D analysis. The tunnel stability value of the MC model is greater with a maximum difference of 98.75% in the 2D analysis and 119.31% in the 3D analysis.
3. Compared to the HB model, the DP model produced exactly the same displacement values in the 2D analysis. However, the tunnel stability value of the DP model is greater with a maximum difference of 98.41% in the 2D analysis.
4. The analysis of initial stress ratio parameter variation resulted in similar deformation values between the HB and DP models and the MC model generated the largest deformation value. For the stability value, the MC model has the highest average stability value among the three models, except for the value of k0 < 0.75 which increases significantly. The DP model has the highest average stability value among the three models except at k0 = 0.33, the DP model has the highest stability value. The HB model consistently had the lowest stability value compared to the other two models, but had the highest gradient of increase in stability value compared to the other models.
5. The analysis of UCS parameter variations resulted in the same deformation value among the three

models, so it can be concluded that the UCS value has no effect on the deformation value of each model. Meanwhile, the stability value of the three models has increased, with the MC model having the highest average stability value among the three models. The DP model produces an average stability value that is in between the MC and DP models with the same increasing gradient as the MC model. The HB model has the lowest average stability value compared to all models with the highest gradient of increase compared to all other models.

ACKNOWLEDGMENT

The authors would like to express their sincere gratitude to Dr. Ir. Herwan Dermawan, M.T., IPM., ASEAN.Eng and Ir. Muhammad Riza H., M.T., IPM., ASEAN.Eng, APEC.Eng from Universitas Pendidikan Indonesia for their invaluable guidance, constructive feedback, and continuous support during the completion of this research. The authors also appreciate all colleagues and peers who provided insightful discussions that enriched this work. The authors would like to thank PT. PLN (Persero) for providing data for this research.

REFERENCES

1. Alejano LR, Bobet A. Drucker-Prager criterion. Rock Mech Rock Eng. 2012 Nov;45(6):995–9.
2. Rafiei Renani H, Martin CD. Slope Stability Analysis using Equivalent Mohr–Coulomb and Hoek–Brown criteria. Rock Mech Rock Eng. 2020 Jan 1;53(1):13–21.
3. Chunyu L, Zhengpeng J, Zhi L, Kefeng X, Bohan W. Analyses on face stability of shallow tunnel considering different constitutive models. Front Mater. 2023 Jan 4;9.
4. Wei Y, Fu W, Ye F. Estimation of the equivalent Mohr–Coulomb parameters using the Hoek–Brown criterion and its application in slope analysis. European Journal of Environmental and Civil Engineering. 2021;25(4):599–617.
5. Chen X, He P, Yan D, Nie A. Face Stability and Reinforcement of the Tunnel in Weak Surrounding Rock. Geotechnical and Geological Engineering. 2020 Oct 1;38(5):5511–21.
6. Xing Y, Kulatilake PHSW, Sandbak LA. Investigation of Rock Mass Stability Around the Tunnels in an Underground Mine in USA Using Three-Dimensional Numerical Modeling. Rock Mech Rock Eng. 2018 Feb 1;51(2):579–97.
7. Rai MA, Kramadibrata S, Wattimena RK. Mekanika Batuan. Penerbit ITB; 2014.
8. Hoek E, Carranza-Torres C, Corkum B, Hoek E, Carranza-Torres C. Hoek-Brown failure criterion-2002 Edition [Internet]. Vol. 1. 2002. Available from: www.rocscience.com.